ORIGINAL ARTICLE
Journal Section

The Earth is Nearly Flat: Precise and Approximate Algorithms for Detecting Vulnerable Regions of Networks in Plane and on Sphere

Balázs Vass[1]* | László Németh[2]† | János Tapolcai[1]*

[1]Department of Telecommunications and Media Informatics, Budapest University of Technology and Economics, Budapest, 1111, Hungary

[2]Department of Probability Theory and Statistics, Eötvös Loránd University, Budapest, 1117, Hungary

Correspondence
Balázs Vass, Department of Telecommunications and media Informatics, Budapest University of Technology and Economics, Budapest, 1111, Hungary
Email: vb@tmit.bme.hu

Funding information
This article is based upon work from COST Action CA15127 (”Resilient communication services protecting end-user applications from disaster-based failures - RECODIS”) supported by COST (European Cooperation in Science and Technology). This work was partially supported by the High Speed Networks Laboratory (HSNLab) at the Budapest University of Technology and Economics, by the BME-Artificial Intelligence FIKP grant of EMMI (BME FIKP-MI/SC), and by the Hungarian Scientific Research Fund (grant No. OTKA FK_17 123957, KH_18 129589, K_17 124171, K_18 128062 and K_17 124171).

Several recent works shed light on the vulnerability of networks against regional failures, which are failures of multiple pieces of equipment in a geographical region as a result of a natural disaster. To enhance the preparedness of a given network to natural disasters, regional failures and associated Shared Risk Link Groups (SRLGs) should be first identified. For simplicity, most of the previous works assume the network is embedded on an Euclidean plane. Nevertheless, they are on the Earth surface; this assumption causes distortion. In this work, we generalize some of the related results on the plane to the sphere. In particular, we focus on algorithms for listing SRLGs as a result of regional failures of circular or other fixed shape.

KEYWORDS
Disaster Protection of Networks, Shared Risk Link Group, Vulnerable Region Detection, Sphere, Computational Geometry.

Abbreviations: SRLG, Shared Risk Link Group; Probabilistic SRLG, PSRLG.

1 | INTRODUCTION

Serious network outages are happening with increasing frequency due to disasters (such as earthquakes, hurricanes, tsunamis, tornadoes, etc.) that take down almost every equipment in a geographical area (see [9] for a recent survey conducted within COST Action RECODIS [21] on strategies to protect networks against large-scale natural disasters). Such failures are called *regional failures* and can have many locations, shapes, and sizes.

Due to the huge importance of telecommunication services, improving the preparedness of networks to regional failures is becoming a key issue [6, 8, 11, 12, 13, 16, 17, 19, 24]. Roughly speaking, protecting networks against regional failures is dealt with either by using geometric tools [2, 7, 19, 25, 26, 27, 30] or by reducing massively the problem space to a set candidate locations of failures [6, 11, 12, 16, 17, 24]. Nevertheless, both approaches require a detailed knowledge of the geometry of the network topology, such as the precise GPS coordinates of nodes and cable conduits' routes, and the statistics of past disasters.

In many works, regional failures are computed by transforming the geographical coordinates of an existing network into a plane, which introduces distortion. Depending both on the geographical area of the network and on the transforming procedure, this distortion can vary from negligible to significant. For example, the backbone network of a small-to-medium size country is not suffering a significant distortion when compared with the uncertainty of the available geographical data, but when turning to networks covering a large country, a continent, or even multiple continents, there is no projection which can hide the spherical-like geometry of the Earth surface (see Fig. 1 taken from [23]). E.g. while the territory of continental US can be mapped onto a plane with 4% distortion [23], if we want to investigate bigger networks, clearly there is no projection which can hide the spherical-like geometry of the Earth.

There are reasons why one should analyze the global communication network as a whole: Electromagnetic storms induced by the Sun's Coronal Mass Ejections (CMEs) could cause severe simultaneous failures of electric and communication networks all over the Earth[1].

Backbone networks are designed to protect a given pre-defined list of failures, called *Shared Risk Link Group*s (SRLGs). Network recovery mechanisms are efficient if this SRLG list covers the most probable failure scenarios while having a manageable size.

An SRLG is called *regional* if it aims to characterize a failure damaging the network only in a bounded geographical area. It is still ongoing research on how to define and compute efficiently regional SRLG lists [25, 26, 30]. A common simplification of these works is that they compute the list of SRLGs on a planar representation of the networks; thus, our focus is to generalize these approaches to the sphere.

An SRLG consists of a set of network links, while node failures are implicitly defined (a node is considered to be failed with the SRLG if all its adjacent edges are part of the SRLG). If a failure f is listed as an SRLG, it is a common approach to skip listing any subset of f (if the network is protected to f, it is also protected to any of its subsets) and, therefore, it is enough to list the maximal SRLGs caused by disasters.

Another issue is that the number of the listed SRLGs has to be kept low. With this aim there is a common practice to fix the shape of the disasters [2, 27] with the assumption that every link intersecting the disaster area is destroyed, while

An earlier version of the paper appeared at IEEE RNDM 2018 [29].

[1] The magnetic storm of 1–2 September 1859 (a.k.a. the Carrington event) was the most intense in the history. It was reported that during this electromagnetic storm, many fires were set by arcing from currents induced in telegraph wires (in both the United States and Europe). It is found that both the Carrington event solar flare energy and the associated coronal mass ejection speed were extremely high but not unique: some predict that the chance of a storm of this or even greater intensity in the next decade is $4-6\%$[15]. In a severe geomagnetic scenario like the Carrington-event, an estimate of $1 trillion to $2 trillion during the first year alone was estimated as the societal and economic costs with recovery times of 4 to 10 years [3]. Electromagnetic storms even smaller than the Carrington event do affect today's networks too: the outage in January 1994 of two Canadian telecommunication satellites during a period of enhanced energetic electron fluxes at geosynchronous orbit, disrupting telecommunication services nationwide. The first satellite recovered in a few hours; recovery of the second satellite took 6 months and cost $50 million to $70 million [3].

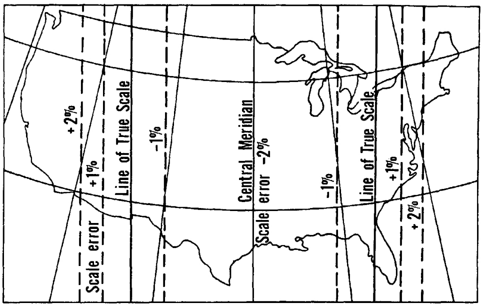

(a) Transverse Mercator Projection

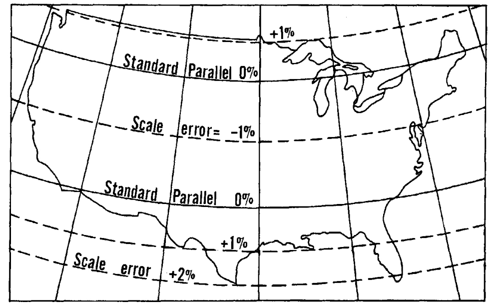

(b) Lambert Conformal Conic Projection

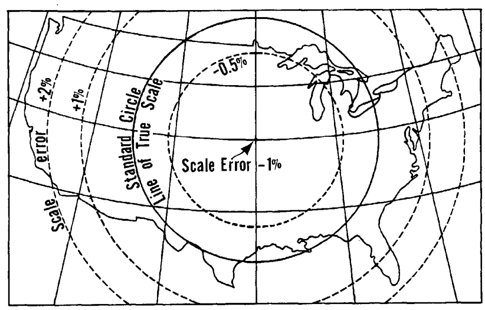

(c) Oblique Stereographic Projection

FIGURE 1 Distortion patterns on common conformal map projections. Projections are shown with a reduction in scale along the central meridian or at the center of projection, respectively. Each of the projections has $> 3\%$ scale error over the US.[23]

the rest of the network is left intact. Among the possible geometric failure shapes, the most natural one is the circular disc, as it is compact, and is invariant to rotation. One possibility is to overestimate the possible failures with circular disks (or any other fixed geometric shape), which yields short SRLG lists. However, it is not clear, what is the cost of this overestimation. In most of this work we choose to overestimate the disasters by circular disks with a maximum size according to one among many possible measures, while we also briefly tackle overestimations with different geometric shapes.

When talking about (maximal regional) disk failures, the most natural measure is the disk radius, which represents the maximum geographical coverage of the natural disaster. Nevertheless, since the network density is usually not homogeneous (i.e., there are more nodes and links in crowded geographical areas than in non-crowded areas) the number of network elements (either nodes or links) contained by the disk are also two useful measures (it is natural that more SRLGs are needed in crowded areas and less crowded areas can be covered with fewer SRLGs). Therefore, in most of this work, we will concentrate on the following three types of SRLG lists:

- *maximal r-range SRLG list*: list of maximal link sets which can be hit by a disk with radius at most r.
- *maximal k-node SRLG list*: list of maximal link sets which can be hit by a disk hitting at most k nodes.
- *maximal k-link SRLG list*: list of maximal link sets which can be hit by a disk hitting at most k links.

To distinguish between lists obtained from planar and spherical representation, we will include attribute *planar* or *spherical* in the list names (e.g. maximal spherical r-range SRLG list) when needed for clarification.

It turns out that in all three mentioned cases, the size of maximal SRLG list is linear in the network size in practice, and can be computed in low polynomial time both in planar case (maximal r-range list: [25], k-node:[30], k-link: [20]) and spherical case.

This paper is an extension of [29], which is, to the best of our knowledge, the first study on enumerating regional SRLG lists in a spherical model. Also, in [29], the first comparison of the spherical and planar representations was provided. It is shown through examples that precise polynomial algorithms could be designed for spherical representation of the networks. In our experience, these algorithms are only 2 times slower than their planar pairs. We also believe that using our approach, resilient routing and network design results [14] can be further enhanced. Compared to the conference version of our paper [29], we have 1) included Subsec. 4.2 presenting approximate algorithms on enumerating the maximal failures induced by arbitrary disaster shapes, 2) provided an enhanced mathematical analysis of algorithms presented Subsections 4.1 and 4.2, 3) and in Sec. 5 added simulation results showing that the difference between the planar and spherical representation of the network can result in different SRLG lists even in case of networks having a geographic extension as small as 100km.

As there are many mathematical derivations in the rest of the paper, we would like to summarize the concepts in plain text once again here for the sake of readability. As learned from previous studies, all of r-range, k-node and l-link lists can be precisely calculated in low polynomial time of the network size in case of planar representation of the network. **Our first goal** was to show that considering spherical embeddings of the networks the possibility of designing low-polynomial time algorithms for determining these SRLG lists remains. We demonstrated this phenomenon in Sec. 3 by designing an algorithm capable of determining the r-range SLRG list both in the planar and spherical case in low polynomial time of the network elements. The existence of fast precise algorithms is good news, however, their drawback is that intuitively the faster the harder they are to implement. This fact motivates our **second goal**, namely designing a framework of simple and fast algorithms capable of determining all the mentioned SRLG lists in both planar and spherical representation with enough precision, which are presented in Subsec. 4.1. Our **third and final goal** is to show how simple approaches can be applied to more general models too: while in most part of this study we concentrated on disasters having a shape overestimated by a disk, Subsec. 4.2 gives an outlook for designing easy-to-implement algorithms for essentially arbitrary disaster shapes.

The remaining of the paper is organized as follows. Sec. 2 describes the network representation model together with the assumptions made. In Sec. 3, we present an example of a polynomial algorithm for computing maximal SRLG list handling both the planar and spherical cases. While in Subsec. 4.1 a faster and more flexible approximate approach is presented for solving the same problem, Subsec, 4.2 gives an outlook for designing algorithms for arbitrary disaster shapes. Simulation results are presented in Sec. 5 and, finally, we draw the conclusions in Sec. 6.

2 | MODEL AND ASSUMPTIONS

Throughout the paper, we will consider two types of embeddings of the network: embedding in Euclidean planar and spherical geometry.

The network is modeled as an undirected connected geometric graph $\mathcal{G} = (V, \mathcal{E})$ with $n = |V| \geq 3$ nodes and $m = |\mathcal{E}|$ edges stored in a lexicographically sorted list. The nodes of the graph are embedded as points in the Euclidean plane or sphere, and their precise coordinates are considered to be given in 2D and 3D Cartesian coordinate system in the planar and spherical case, respectively. Note that if coordinates are given in polar system (in case of spherical

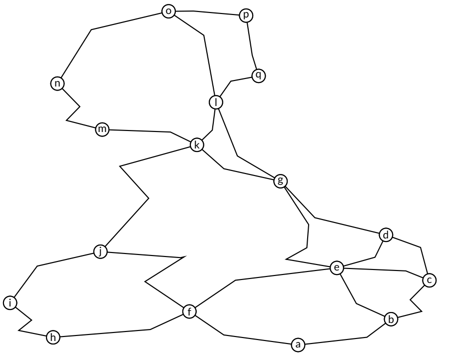

FIGURE 2 Input graph $\mathcal{G}(V, \mathcal{E})$ with polylines, $n = 17, \gamma = 4$

geometry), one can easily transform them to Cartesian at the very beginning.

When speaking of planar geometry, for each edge e there is a *polygonal chain* (or simply *polyline*) e^l in the plane in which the edge lies (see Fig 2). Parameter γ will be used to indicate the maximum number of line segments a polyline e^l can have. Naturally, in spherical case, the polyline of an edge refers to a series of geodesics. Note that this model covers special cases when edges are considered as line segments (geodesics).

It will be assumed that basic arithmetic functions $(+, -, \times, /, \sqrt{\ })$ have constant computational complexity. For simplicity, we assume that nodes of V and the corner points of the containing polygons defining the possible route of the edges are all situated in general positions of the plane, i.e. there are no three such points on the same line and no four points on the same circle, and in the spherical case there are no antipodal nodes or breakpoints and no great circles of geodesics of polylines cross the North pole.

In this study, our goal is to generate a set of SRLGs, where each SRLG is a set of edges. Note that from the viewpoint of connectivity, listing failed nodes besides listing failed edges has no additional information. We consider SRLGs that represent worst-case scenarios the network must be prepared for and, thus, there is no SRLG which is a subset of another SRLG.

2.1 | Model for Circular Disk Shaped Disasters

In most of this study, it will be assumed that disasters are either having a shape of a circular disk or they are overestimated by a circular disk.

We will often refer to circular disks simply as disks. The disk failure model is adopted, which assumes that all network elements that intersect the interior of a circle c are failed, and all other network elements are untouched.

Definition A circular disk failure c hits an edge e if the polyline of the edge e^l intersects disk c. Similarly node v is hit by failure c if it is in the interior of c. Let $\mathcal{E}_c$ (and V_c) denote the set of edges (and nodes, resp.) hit by a disk c.

We emphasize that in this model when we say e is hit by c, it does not necessarily mean that e is destroyed indeed by c, instead, it means that there is a positive chance for e being in the destroyed area. In other words, this modeling technique does not assume that the failed region has a shape of a disk, but overestimates the size of the failed region in order to have a tractable problem space.

Notation	Denomination	Short name
M_r^p	maximal planar r-range SRLG list	planar r-range list
M_k^p	maximal planar k-node SRLG list	planar k-node list
M_l^p	maximal planar l-links SRLG list	planar l-link list
M_r^s	maximal spherical r-range SRLG list	spherical r-range list
M_k^s	maximal spherical k-node SRLG list	spherical k-node list
M_l^s	maximal spherical l-links SRLG list	spherical l-link list

TABLE 1 Notations and denominations of the list types

Definition Let $\mathcal{C}^p$ and $\mathcal{C}^s$ denote the set of all disks in the plane and the set of all disks on the sphere, respectively. For both geometry types $g \in \{p, s\}$, let $\mathcal{C}_r^g$, $\mathcal{C}_k^g$ and $\mathcal{C}_l^g$ denote the set of disks part of $\mathcal{C}^g$ having radius at most r, hitting at most k nodes of V and hitting at most l links of $\mathcal{E}$, respectively.

Based on the above definition, we define the set of failure states that a network may face after a disk failure, with a maximal measure.

Definition For all geometry types $g \in \{p, s\}$ and SRLG type $t \in \{r, k, l\}$, let set $F(\mathcal{C}_t^g)$ denote the set of edges which can be hit by a disk $c \in \mathcal{C}_t^g$, and let $M_t^g = M(\mathcal{C}_t^g)$ denote the set of maximal edge sets in $F(\mathcal{C}_t^g)$.

Table 1 gives an overview on the corresponding notations and denominations of the SRLG list types we focus on on this paper. Note that for every SRLG type $t \in \{r, k, l\}$ if $f \in M_{t=s}^g$ there is an $f' \in M_{t=s'}^g$, such that $f \subseteq f'$ where $s \leq s'$.

One aim of this study is to propose fast algorithms computing these lists for various sizes of m.

2.2 | Model for Disasters with Arbitrary Shape

In Subsec. 4.2 we give an outlook for simple algorithms handling disasters which have a shape of a fixed non-self-intersecting closed polytope in the plane having boundaries consisting of line segments and arcs. The disaster can occur in any physical area and with any orientation. A link is hit is it has at least a common point with the disaster. The model is basically the same as the one described in the previous Subsec., the only difference is the disaster shape.

3 | PRECISE ALGORITHMIC APPROACHES FOR ENUMERATING MAXIMAL FAILURES

As mentioned before, determining the planar lists M_r^p, M_k^p, M_l^p is relatively well studied. It remains a question of how much the distortion of maps can affect the calculated SRLG lists. The answer is that it heavily depends on the projection used to make the map. For example, while the *stereographic projection* affect significantly the distances, but in contrast to many other projections it has the nice property of mapping spherical disks to planar disks [22] (fact also used in Appendix .1). One approach for calculating spherical lists would be to adapt existing algorithms to spherical geometry demonstrating the interoperability between these geometries. However, in this paper, we follow an approach simpler to

Algorithm 1: Refreshing M with failure f

Input: M, f
Output: M refreshed with f
begin

```
maximal:=True
for f_M ∈ M do
    if f ⊆ f_M then
        maximal:=False
if maximal then
    M := M ∪ {f}
    for f_M ∈ M do
        if f ⊃ f_M then
            M := M \ {f_M}
return M
```

present and avoiding trigonometric calculations via applying the projection in both directions for numerous times. In other words, some steps of the algorithm are performed on the plane, while others on the sphere.

In the followings, we extend a precise algorithm for determining M_r^p (see [25]) to an algorithm computing M_r^p or M_r^s depending on the geometry of the input. In the rest of this section, we present this extended algorithm.

3.1 | Smallest Enclosing Disks

Let us make the following definition for the sake of clarifying the intuition.

Definition Let a disk c be smaller than disk c_0, if c has a smaller radius than c_0, or if they have an equal radius and the center point of c is lexicographically smaller than the center point of c_0. Among a set of circles S_c, let c be the smallest if it is smaller than any other circle in S_c.

Definition Let $F \subseteq E$ be a finite nonempty set of edges (not necessarily a failure). We denote the smallest disk among the disks enclosing the polylines of F by c_F and we say c_F is the smallest enclosing disk of F.

It is not difficult to see that c_F always exists for line segments or geodesics (depending on the geometry), and thus, by mapping the corresponding segments/geodesics together we can deduct that the definition is correct for polylines too. The key idea of our approach is that we can limit our focus only on the smallest enclosing disks c_F. The consequence of the next proposition is that the number of smallest enclosing disks c_F is not too large.

Proposition 1 *Let H be a nonempty set of polylines of edges with smallest enclosing disk c_H. Then there exists a subset $H_0 \subseteq H$ with $|H_0| \leq 3$ such that $c_H = c_{H_0}$.* ■

Definition Let $\mathcal{S}$ denote the set of maximal edge sets hit by a smallest enclosing disk.

By Prop. 1 we have:

Corollary 2 $|\mathcal{S}| \leq \binom{m}{3} + \binom{m}{2} + m = \frac{m^3}{6} + \frac{5m}{6}$. ■

Algorithm 2: Determining maximal r-range SRLG lists

Input: $\mathcal{G}(V, \mathcal{E})$, r, geometry g, coordinates of nodes and edge polylines
Output: M_r^g
begin
  $M_r^g := \emptyset$
  Store $\mathcal{E}$ as a list,
  for $i_1 \in \{1, \ldots, m\}$ **do**
    for $i_2 \in \{i_2, m\}$ **do**
      for $i_3 \in \{i_3, m\}$ **do**
        $c_{i_1,i_2,i_3} := c_{\{\mathcal{E}[i_1],\mathcal{E}[i_2],\mathcal{E}[i_3]\}}$
        if *radius of* c_{i_1,i_2,i_3} *is* $\leq r$ **then**
          $f := F(c_{i_1,i_2,i_3})$
          refresh M_r^g with f `// as in Alg. 1`
  return M_r^g

Lemma 3 *Let H be a set of line segments in the plane or geodesics on the sphere, $|H| \leq 3$. Then c_H can be determined in $O(1)$ time.*

The proof of the Lemma is relegated to the Appendix .1.

Theorem 4 *Let H be a set of polylines of edges, $|H| \leq 3$. Then c_H can be determined in $O(\gamma^3)$ time.*

Proof First, unpack each polyline into the $\leq \gamma$ line segments/geodesics it is consisting of. Then, for each element h_i in H, pick a segment s_i. For each triplet (couple) of segments calculate the smallest enclosing disk (which by Lemma 3 can be done in $O(1)$), and lastly chose the smallest from among the resulting disks.

3.2 | Polynomial algorithm for determining maximal failures

In this subsection, we repeat an extension of the basic algorithm provided by [25] which handles both spherical and planar inputs. There are two key facts inspiring this algorithm. Firstly, based on Prop. 1:

Corollary 5 (of Prop. 1) *For both $g \in \{p, s\}$ and every $f \in M_r^g$ there exist $\{e_1, e_2, e_3\} \in f$ such that $c_{\{e_1,e_2,e_3\}} = c_f$.*■

Secondly, according to Theorem 4, smallest enclosing disks can be computed in $O(\gamma^3)$ both in the plane and on the sphere. Based on these, Alg. 2 is presented, which is a straightforward basic polynomial algorithm. Here, the key idea is to maintain a list M' of maximal failures detected so far while scanning through the link sets f covered by the smallest enclosing disks of at most 3 edges. If there is no $f_M \in M'$ containing f, then f is appended to M' and all $f_M \in M'$ which are part of f are removed as presented in Alg. 1. This process is called *refreshing*.

The following theorem gives a very loose bound on the complexity of calculating M_r^g.

Theorem 6 *Alg. 2 computes M_r^g in $O(m^3(\gamma^3 + m^4))$. M_r^g has $O(m^3)$ elements.*

Proof Based on Prop. 1 the algorithm is correct, it is computing M_r^g. There are $O(m^3)$ smallest enclosing disks to calculate, each in constant time. We claim that for each disk the calculation time of refreshing M_r^g with the resulting failure (according to Alg. 1) is $O(m^4 + \gamma^3)$ in case of each disk, because after the computation of the smallest enclosing disk in $O(\gamma^3)$ and determining f in $O(m)$ there has to be done $O(m^3)$ comparisons of link set, and each can be done in $O(m)$.

3.3 | On improved complexity bounds

The results from the previous subsection can be easily improved using parametrization and some computational geometric tricks.

The first observation is that for any meaningful radius of the disk failure most of the network will remain intact. However, failures with the same radius taking place in a crowded area tend to take down more equipment than the ones in sparsely inhabited areas. This motivates the introduction of a graph density parameter:

Definition For every $r \in \mathbb{R}_0^+$, let ρ_r be the maximum number of edges which can be destroyed by a disk with radius at most r.

This ρ_r is considered to be small in case of small r values. Another observation is that there are not much more network edges than nodes. This is formalized in the upcoming Claim 1.

Informally speaking, we denote the set of crossing points of the edges by X. A more formal definition follows.

Definition Let X be the set of points P in the plane on which no node element of V lies and there exist at least 2 edges which have polylines having a finite number of common points crossing each other in P. Let $x = |X|$.

Despite the fact that on arbitrary graphs x can be even $O(n^4)$, in backbone network topologies typically $x \ll n$ because a node is usually installed if two cables are crossing each other. This gives us the intuition that G is 'almost' planar, and thus it has few edges.

Claim 1 *The number of edges in G is $O(n + x)$. More precisely for $n \geq 3$ we have $m \leq 3n + x - 6$.*

Proof If $\mathcal{G}$ is embedded in the plane, do the followings. Let $G_0(V \cup X, E_0)$ be the planar graph obtained from dividing the polylines of edges of G at the crossings. Since every crossing enlarges the number of edges at least with two, $|E_0| \geq m + 2x$. On the other hand, $|E_0| \leq 3(n + x) - 6$ since G_0 is planar. Thus $m \leq |E_0| - 2x \leq 3n + x - 6$.

If $\mathcal{G}$ is embedded in the sphere, we can project it to the plane with stereographic projection, repeat the former arguments then apply an inverse projection to the sphere.

A third trick lies on the fact that in practice $|M_r^g|$ is $O(n)$ (as presented in planar case in [25]), thus in Alg. 1 typically there has to be done only $O(n)$ comparisons. Thus we introduce a third parameter:

Definition Let λ be the maximum cardinality of the list of maximal failures detected so far in Alg. 2, 3 and 4, respectively.

Combining the former three observations lower parametrized complexity can be achieved:

Theorem 7 *Alg. 2 computes M_r^g in $O((n + x)^3(n + x + \lambda\rho_r + \gamma^3)$.*

Proof Based on Prop. 1 the algorithm is computing M_r^g. There are $O((n + x)^3)$ smallest enclosing disks to calculate, each in constant time. We claim that for each disk the calculation time of Alg. 1 is $O((n + x)^3\rho_r + \gamma^3)$ in case of each disk, because after the computation of the smallest enclosing disk in $O(\gamma^3)$ and determining f in $O(n + x)$ there has to be done $O(\lambda)$ comparisons of link set, and each can be done in $O(\rho_r)$.

Corollary 9 will give more intuitive bounds on the running time of Alg. 2.

Definition Let *diam* be the geometric diameter of the network.

Proposition 8 *Based on simulation results from Sec. VI. of [25], in case of backbone networks, ρ_r is proportional to $\frac{2r}{diam}$ in the interval $(0, diam/2]$, where diam is the geometric diameter of the network.*

Corollary 9 (cor. of Thm. 7) *If both x and λ is $O(n)$, Alg. 2 computes M_r^g in $O(n^3(n\rho_r + \gamma^3))$ time. If, in addition, γ is $O(1)$ and ρ_r is $O(r/diam)$, Alg. 2 computes M_r^g in $O(n^4 \frac{r}{diam})$ time.*

Cor. 9 proposes that M_r^g can be determined in quartic time of n in practice. On the other hand, Alg. 2 has its limits of speed: because of the three nested for-loops, it runs in $\Omega(n^3)$. In order to achieve better results, the algorithm would have to be changed. For the planar case, [25] gives an algorithm which runs in $O((n + x)^2\rho_r^5)$ for $\gamma = 1$ (i.e. the edges are considered as line segments there). Furthermore, we are convinced that an algorithm with parametrized running time near linear in network size could be achieved for determining M_r^g (and also for determining M_k^g and M_l^g, despite they can be computed based on very different theories). However, presenting this kind of algorithms would exceed the limits of this paper.

4 | APPROXIMATE ALGORITHMS AND IMPLEMENTATION ISSUES

It is always good to have fast precise polynomial algorithms for solving a given problem. However, this approach also has some disadvantages: 1) the lower complexity a precise algorithm for determining a maximal circular SRLG list has, the harder to implement and prove its correctness and complexity; 2) designing algorithms for computing different types of maximal SRLG lists need totally different mathematics. Moreover, in most cases, the available geographical data of networks is inaccurate. Adding this fact to the inconveniences of the precise approach results into the idea of designing some approximate algorithms that are able to compute these lists *with enough precision*.

The main idea behind this class of algorithms that instead of keeping the original shape and size of the disaster area and taking in count all the infinitely many possible disaster centers, we slightly overestimate the disaster letting us detect all the same (or occasionally a bit larger) hit link sets while going through only a finite number of centers.

4.1 | Approximate algorithms for circular disk failures

In this section, we present an approximate approach suitable for computing all types of maximal SRLG lists defined in Sec. 2.

Definition For a point P (in the plane or on the sphere) and node $v \in V$, let the node-distance couple be $[v, d(v, P)]$, where $d(v, P)$ is the distance of v and P. Let $e(P)$ be the list consisting of the link-distance pairs of all links $e \in \mathcal{E}$, sorted according to the lexicographical order of the links. Let $e(P)_{\text{hit}}$ be the sorted list of links not further from P than r.

Proposition 10 *For a given point P, both $e(P)$ and $e(P)_{\text{hit}}$ can be computed in $O((n + x)\gamma)$.* ■

Clearly, both node-distance lists and edge-distance lists can be determined quickly. The plan is to determine these lists for enough points which are also placed well enough to be able to determine the maximal SRLG lists based on these node-distance and edge-distance lists.

Definition Let $\mathcal{P}$ denote the set of points P for which we want to construct the link-distance lists $e(P)$.

Algorithm 3: Approximate algorithm for determining the maximal r-range SRLG lists

Input: $\mathcal{G}(V, \mathcal{E})$, r, $\mathcal{P}$, geometry type g, coordinates of nodes and polylines of edges
Output: M_r^g
begin
  for $P \in \mathcal{P}$ **do**
    determine $e(P)_{\text{hit}}$
    if $e(P)_{hit} \neq \emptyset$ **then**
      refresh M_r^g with $e(P)_{\text{hit}}$ `// according to Alg. 1`
  return M_r^g

Let us stick to planar geometry for a moment. Intuitively, we can calculate M_r^p by including the grid points of a sufficiently fine grid (let's say containing 1 km $\times$ 1 km squares) in $\mathcal{P}$. On the sphere, we should choose a similar nice covering. It is possible that we have some extra short links, thus for calculating the k-node and k-link list we should include some extra points in $\mathcal{P}$. For example, by adding some random points of each polyline of edge and some point near every node we can solve this issue.

Definition Let $d_{\mathcal{P}}$ be the maximal distance of any geometric location from the (closed) convex hull of the geometric embedding of graph G to the closest point of set $\mathcal{P}$, i.e. $d_{\mathcal{P}} := \max_{t \in \text{conv}(G)} \min_{p \in \mathcal{P}} \text{dist}(p, t)$.

Definition Taken two set of sets E_1 and E_2, we denote the relationship of the sets with $E_1 \sqsupseteq E_2$ if and only if for all $e_2 \in E_2$ there exists an $e_1 \in E_1$, such that $e_1 \supseteq e_2$.

Algorithm 3 is an example approximate algorithm for determining M_r^g.

Theorem 11 *The resulting list H_r^g of running Alg. 3 is determined by the algorithm in $O(|\mathcal{P}|[(n+x)\gamma + \lambda\rho_r])$. Furthermore, $M_r^g \sqsupseteq H_r^g \sqsupseteq M_{r-d_P}^g$.*

Proof Regarding to the complexity, for an element P of $\mathcal{P}$ we have to construct $e(P)_{\text{hit}}$, which can be done in $O((n+x)\gamma)$, then refresh the list of suspected maximal failures with $e(P)_{\text{hit}}$ in $O(\lambda\rho_r)$, since the list constains at most λ ordered lists consisting of at most ρ_r edges.

On the other hand, $M_r^g \sqsupseteq H_r^g$ is immediate, since the algorithm investigates only a subset of disks with radius r, while for every point t in the r-neighbourhood of conv(G), there exists a $p \in \mathcal{P}$ such that disk $c(t, r - d_{\mathcal{P}}) \subseteq c(p, r)$, yielding $H_r^g \sqsupseteq M_{r-d_P}^g$, from where the proof follows.

Using the fact that the shape of the disasters is a closed disk we get the following corollary:

Corollary 12 $\lim\limits_{d_{\mathcal{P}} \to 0} H_r^g = M_r^g$*, for any fixed network.*

Corollary 13 (of Thm. 11) *$M_r^g \sqsupseteq H_r^g \sqsupseteq M_{r-d_P}^g$. Furthermore, if both of x and λ is $O(n)$, the resulting list H_r^g of running Alg. 3 is determined by the algorithm in $O(|\mathcal{P}|n(\gamma + \rho_r))$. If in addition, γ is $O(1)$, and ρ_r is $O(r/diam)$, H_r^g is determined by Alg. 3 in $O(|\mathcal{P}|n\frac{r}{diam})$.*

Based on Thm. 11, if one wants to protect disasters caused by disks with radius r, it is only needed to run Alg. 3 initializing the radius as $r + d_{\mathcal{P}}$.

Comparing Cor. 13 and 9 we can see that despite the approximate Alg. 3 is much simpler to implement, and taking in count that disasters are not precisely circular and the chosen radius is arbitrary, it clearly outperforms the precise Alg. 2.

4.2 | Approximate algorithms for disasters with arbitrary shape

Understanding how to deal with circular disk failures is a good start, however, one should consider other disaster shapes too. In [28] it is proven that there is a polynomial number of maximal failures caused by disasters having elliptic or polygonal (e.g. rectangular or equilateral triangular) shape. Again, as engineering fast precise algorithms for determining SRLG lists similar to M_r, M_k or M_l but for arbitrary disaster shape instead of a circle is not trivial, we are going to discover the possibilities of approximate algorithms similar to the one described for determining M_r. In short, while the disk is invariant to rotation, now one should consider also the different orientations of the fixed shape. We shall discretize the continuous rotation of the shapes via taking only a possible orientations if the shape:

Definition Let F_r be a set of non-self-intersecting closed polytopes embedded in the plane having boundaries consist of line segments and arcs, for which 1) every $f_1, f_2 \in F_r$, f_1 can be moved into f_2 via a translation and a rotation, 2) the smallest fitting disk of any $f \in F_r$ has a radius of r.

Let $N_{d_\mathcal{P}}(F_r)$ be consisting of the elements f of F_r, each f extended (as $f' := N_{d_\mathcal{P}}(f)$) with the smallest $d_\mathcal{P}$-neighborhood of f.

Let T be an arbitrary point of a polytope $f \in F_r$. Let $N(F_r) = N_{d_\mathcal{P}+d_{a,T}}(F_r)$ be the consisting of the elements f' of $N_{d_\mathcal{P}}(F_r)$, each f' extended as f'' with the smallest $d_{a,T}$-neighborhood of f' (where distance $d_{a,T}$ is a function of the extended shape f', the number of orientations of the shape considered a, and the center of rotation $T \in \text{int} f$) in such way that:

$$\bigcup_{z\in[0,2\pi)} \texttt{rotate}(f', T, z) \subseteq \bigcup_{z\in\{0,\frac{2\pi}{a},\dots,\frac{2(a-1)\pi}{a}\}} \texttt{rotate}(f'', T, z). \tag{1}$$

Note that by the former definition for any possible place and orientation of a disaster with shape f, in which f intersects at least a network element, there exists a $p \in \mathcal{P}$ and an orientation (out of the a investigated orientations) of the extended disaster shape f'' for which the area destroyed by f'' is containing the area destroyed by f, thus the edge set hit by f'' is a superset of the edge set hit by f.

Proposition 14 $\lim_{\substack{d_\mathcal{P}\to 0\\ a\to\infty}}(d_\mathcal{P} + d_{a,T}) = 0$.

Definition Let ϕ denote the number of line segments and arcs needed to describe a shape from F_r. Let ϱ_r be the maximal number of edges an $f \in F_r$ can hit.

Definition For geometry type $g \in \{p, s\}$, let denote the set of maximal failures caused by disasters from F_r and $N(F_r)$ by $M^g_{F_r}$ and $M^g_{N(F_r)}$, respectively.

Algorithm 4 is an example approximate algorithms for determining $M^g_{F_r}$.

Theorem 15 *The resulting list $M^g_{N(F_r)}$ of running Alg. 4 is determined by the algorithm in $O(|\mathcal{P}|a[\phi + (n + x)(\phi + \frac{\log|\mathcal{P}|}{a})\gamma + \lambda\varrho_r)])$ if the original failure shape f is convex. Furthermore, for any given network, $\lim_{\substack{d_\mathcal{P}\to 0\\ a\to\infty}} M^g_{N(F_r)} = M^g_{F_r}$.*

Proof Clearly, the algorithm computes $M^g_{N(F_r)}$.Based on Prop. 14 proposing that as $d_\mathcal{P} \to 0$ and $a \to \infty$, the necessary inflation of the original shape f tends to 0, we also can see that for any given network, $\lim_{\substack{d_\mathcal{P}\to 0\\ a\to\infty}} M^g_{N(F_r)} = M^g_{F_r}$.

Regarding its complexity, we can argue as follows.

Algorithm 4: Approximate algorithm for determining $M^g_{F_r}$ (the maximal failures the disaster shape f can cause)

Input: $\mathcal{G}(V,\mathcal{E})$, r, F_r, a, $\mathcal{P}$, geometry type g, coordinates of nodes and polylines of edges
Output: $M^g_{R(F_r)}$
begin
1 Calculate $d_{\mathcal{P}}$
2 Let $f \in F_r$, calculate f'' according to the definition of $N(F_r)$
3 **for** $P \in \mathcal{P}$ **do**
4   translate f'' such that $T = P$ `// T is a fixed interior point of f''`
5   **for** $z \in \{0, \frac{2\pi}{a}, \ldots, \frac{2(a-1)\pi}{a}\}$ **do**
6     $f_z := \mathtt{rotate}(f'', T, z)$
7   refresh $M^g_{N(F_r)}$ with $\{e \in E \mid f_z \cap \text{polyline of } e \neq \emptyset\}$ `// according to Alg. 1`
8 **return** $M^g_{N(F_r)}$ `//` $\simeq M^g_{F_r}$`, i.e. the maximal failures the disaster shape f can cause`

To calculate $d_{\mathcal{P}}$, we observe that all the points in $N_r(G)$ (the smallest r-neighborhood of the convex hull of G) maximizing the distance from $\mathcal{P}$ lie on the intersection of at least 3 Voronoi cells computed on point set $\mathcal{P}$, restricted to $N_r(G)$, and the outer region of $N_r(G)$ taken as an extra cell. The Voronoi regions of $\mathcal{P}$ can be computed in $O(|\mathcal{P}|\log|\mathcal{P}|)$ time both in the plane and on the sphere (plane: Section 7.2 in [5], sphere: special case of Corollary 2 in [18]). Using Claim 1, one can see that the number of line segments and arcs (or geodesics on the sphere) needed to describe $N_r(G)$ is $O((n+x)\gamma)$, thus we claim the total complexity of computation and description the modified Voronoi diagram described before is $O((n+x)\gamma|\mathcal{P}|\log|\mathcal{P}|)$. Based on the graph representation of the diagram one can determine $d_{\mathcal{P}}$ in the proposed complexity.

We claim that line 2 can be done in $O(\phi)$ if f is convex. In case of non-convex failure shapes f calculations can become more compicated (e.g. holes in f can dissapear in f''), but clearly, f'' can be determined in polynomial time of ϕ in this case too.

For a given $P \in \mathcal{P}$, translation of f (Line 4) can be done in $O(\phi)$.

For a given $P \in \mathcal{P}$ and $z \in \{0, \frac{2\pi}{a}, \ldots, \frac{2(a-1)\pi}{a}\}$, rotation (Line 6) can be done in $O(\phi)$.

For a given point and direction, line 7 needs $O((n+x)\phi\gamma + \lambda\varrho_r)$ of computation, as follows. For every edge $e \in \mathcal{E}$ one has to check whether its polyline e^l intersects the boundary of f_z or if not, is e^l situated entirely in f_z, both can be checked in $O(\phi\gamma)$. Then, refreshing $M^g_{N(F_r)}$ with the edge set hit by f_z can be done in $O(\lambda\varrho_r)$, since edges are stored in ordered lists.

We can conclude that Algorithm 4 is correct and runs in the proposed complexity.

Algorithm 4 clearly runs in polynomial time of the input size (even for non-convex disaster shapes f), and can be applied for a wide variety of disaster shapes.

Corollary 17 will offer a more intuitive complexity result on Alg. 4:

Proposition 16 *Since any $f \in F_r$ can be covered with a disk having a radius r, $\varrho_r \leq \rho_r$. Based on Prop. 8, this also means that ϱ_r is $O(\frac{r}{diam})$ in case of backbone networks.*

Corollary 17 *If the number of edge crossings x is $O(n)$, parameters γ and ϕ are $O(1)$, and $\log|\mathcal{P}|$ is chosen to be $O(a)$, the resulting list $M^g_{N(F_r)}$ of running Alg. 4 is determined by the algorithm in $O(|\mathcal{P}|a(n+\lambda\varrho_r))$. If, in addition, λ is $O(n)$, and ϱ_r is $O(\frac{r}{diam})$, the runtime is $O(a|\mathcal{P}|n\frac{r}{diam})$.*

If we compare Cor. 17 and 13, we can see that unless the shape f of disasters is very complicated, the only real additional complexity compared to the circular disk failure case arises from the fact that that usually f is not invariant to rotation.

Comparing Cor. 17 and 9 we can see that despite the approximate Alg. 3 handles the much more complex problem induced by disasters having an arbitrary given shape f, it has a lower complexity compared to the precise Alg. 2 dealing with only circular disasters, showing the strength of the proposed framework of approximate algorithms.

5 | SIMULATION RESULTS

In this section, we present numerical results that validate our approximate approach for circular disk failures presented in Subec. 4.1, and demonstrate the use of the proposed algorithms on some realistic physical networks. The algorithm was implemented in Python3.5 using various libraries. Distance functions were implemented from scratch. No special efforts were made to make the algorithm space or time optimal. Run-times were measured on a commodity laptop with Core i5 CPU at 2.3 GHz with 8 GiB of RAM. The output of the algorithm is a list of SRLGs so that no SRLG contains the other.

We interpret the input topologies in two ways: *polygon*, where links are polygonal chains, and *line*, where the corner points of the polygonal links are substituted with nodes (of degree 2). Here links are line segments.

5.1 | Extreme Geographical Extension Makes Difference

We found that running times for spherical representations were ~ 2 times slower than the planar ones in case of most networks (see Table 2). The only exception is when the network has an extreme geographic extension (e.g. AboveNet), in this case, the obtained SRLG lists tend to be longer (Fig. 3 demonstrates this in case of k-link lists) causing a slight increase both in parameter λ and in the running time.

Another issue which can be noticed related to the achievable preciseness using the approximate approach. Based on Thm. 11, running time is proportional with $|\mathcal{P}|$; given this and the running times collected in Table 2, we can deduce that if the drop of price of computation power remains for an additional short time period, one will be able to run these simulations even at home for huge $|\mathcal{P}|$ (e.g. $|\mathcal{P}| \simeq 5 * 10^8$, which number is approximately the Earth's surface in $\mathtt{km}^2$), yielding a high precision. Note that Alg. 3 could be easily parallelized.

TABLE 2 Running times of Alg. 3 on some physical backbone topologies of [1] (in *sec*, $|\mathcal{P}| \simeq 50000$)

Name	$\lvert V \rvert$		$\lvert \mathcal{E} \rvert$		Planar runtime		Spherical runtime	
	Polygon	Line	Polygon	Line	Polygon	Line	Polygon	Line
AboveNet	9	22	15	28	232	156	410	757
LambdaNet	10	33	10	33	282	225	444	410
GARR (Italy)	16	16	18	18	107	92	204	187
GTS (Hungary)	14	15	39	26	175	146	311	291

The k-link list is chosen as an illustrative example on Fig. 3. In Fig. 3a and 3b we can see that for $k = 1$ there are listed all the single link failures. For $k \geq 2$ there is a higher chance on the sphere for k links to be 'close' to each

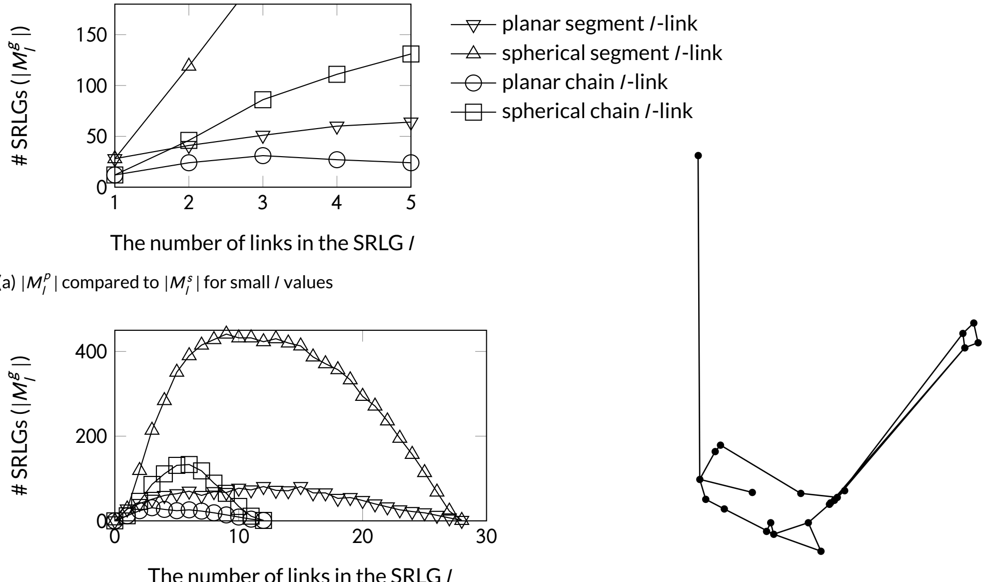

(a) $|M_l^p|$ compared to $|M_l^s|$ for small l values

(b) $|M_l^p|$ compared to $|M_l^s|$ for for all possible l values

(c) Best Mercator projection of AboveNet

FIGURE 3 Example on extreme geographic extension: AboveNet ($n = 22$, $m = 28$ in *line* case) touching three continents.

other than on the plane, thus $|M_l^s| > |M_l^p|$. This phenomenon might appear because mapping the sphere to the plane intuitively lets fewer edges to be next or close to each other. As the number of links in the SRLGs l increases, $|M_l^g|$ first increases too, then after plateauing it starts to decrease, which is just a rephrasing of the intuition that there are the most possible scenarios of a disk hitting exactly l links when $l \simeq m$. Finally, $|M_m^g| = 1$, because there is only one possibility of hitting all the links.

The obtained SRLG lists are different for the two geometries, thus it makes sense to use the much precise spherical model.

5.2 | Cardinality of SRLG lists Induced by Disasters with a Shape of Circular Disk

In this subsection a brief overview is given on the typical cardinality of the proposed (planar) l-link, k-node and r-range lists. The chosen example topology is the `28_optic_eu` drawn in Subfig. 4c, and having 19 and 28 vertices, and 32 and 41 edges, in *polygon* and *line* case, respectively. On Subfig. 4b. one can see that all of $|M_l^p|$, $|M_k^p|$ and $|M_r^p|$ is reasonably small, for smaller values of the measure.

$|M_{l=1}^p|$ equals the number of edges by definition, and for $l \in \{1, \ldots 5\}$, $1.2 * l$ times the number of edges is a good approximation for the cardinality of the list. This linear increasement then flattens out, $|M_l^p|$ reaching its maximum at $l = 10$ and 15 in *chain* and *line* case, respectively, then slowly decreases to 1, while l reaches the number of edges.

The overall dynamics of graphs of $|M_k^p|$ are the same that of $|M_l^p|$, however, the increasement in the number of SRLGs is more moderate for small k values: $(k + 1.2)$ times the number of nodes is a good approximation for $|M_k^p|$ in the area of small k values, and the cardinality culminates at $|M_{k=6}^p| = 78$ and $|M_{k=8}^p| = 142$ in chain and segment case, respectively.

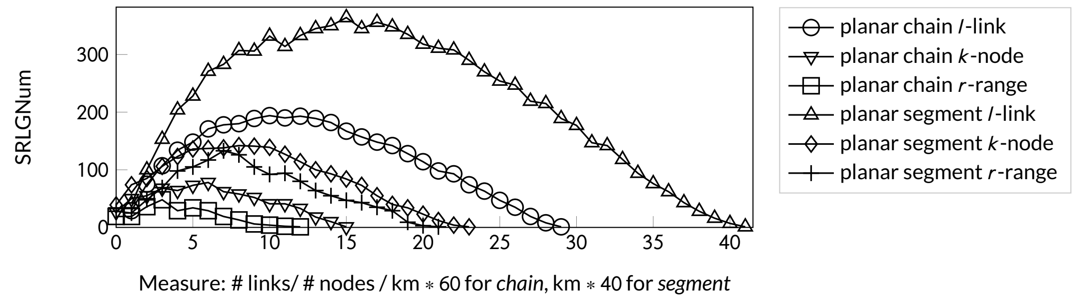

(a) $|M_l^p|$ compared to $|M_n^p|$ and $|M_r^p|$ for all possible l / k / r values.

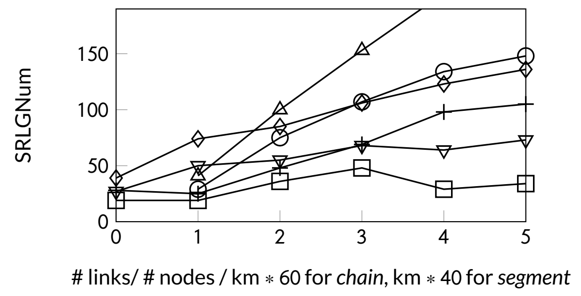

(b) $|M_l^p|$ compared to $|M_n^p|$ and $|M_r^p|$ for small l / k / r values.

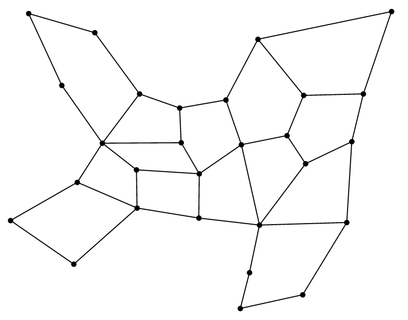

(c) A planarization of 28_optic_eu

FIGURE 4 Example on list behaviors: `28_optic_EU` ($|V|$ is 19 and 28, $|\mathcal{E}|$ is 32 and 41, in *polygon* and *line* case, respectively.)

It is easy to see that $|M^p_{r=0}|$ equals to the number of nodes and edge crossings, the worst places of disasters having small geographical extensions being at nodes and edge crossings. In case of this topology and the chosen radiuses, the maximum cardinality of M_r^p was reached at 180km and 280km for chain and segment case, respectively, with values of 48 and 133.

5.3 | When can we Negligate the Curvature of the Earth?

An important question is that, in practice, under which geographic extension of the network can one say that, in the viewpoint of SRLG enumeration, it is practically indifferent whether we consider a spherical or a planar representation of the network. In other words, focusing now only on lists M_r, the question is that under which size of the physical network will M_r^p and M_r^s (maximal link sets which can be hit by a single circular disk with radius r, in the plane and on the sphere, resp.) be the precisely the same. The answer depends not only on the physical size, but also on the specialties of the network itself: it can represent dense metropolitan backbone network with multiple nodes close to each other, but it can also be geographically very sparse. Keeping in mind that in metropolitan areas there can be much more differences, we took network `AboveNet` (Fig. 3c), and its shrunk instances, where `AboveNet/c` means that we rotated `AboveNet` such that the average lat and lon coordinates to be both 0, then we divided each coordinate by c. We were interested in the smallest possible shrinking ratio, for which $M_r^p = M_r^s$.

We used $\mathcal{M}(r) := |M_r^p \triangle M_r^s|/(|M_r^p| + |M_r^s|) \in [0,1]$ (the ratio of SRLGs, which are present in only one of M_r^p and

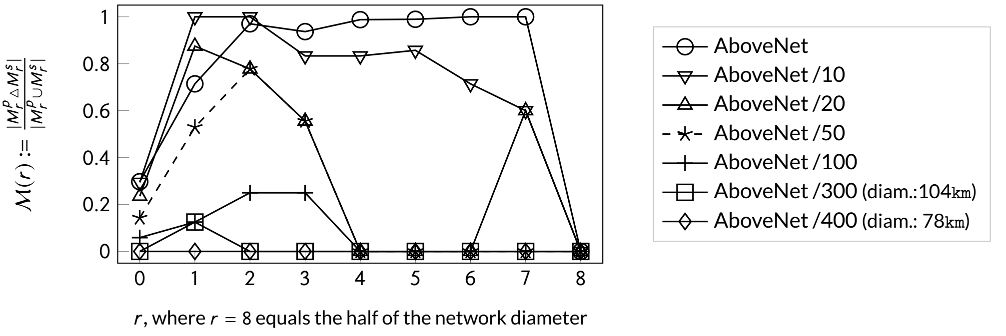

FIGURE 5 The ratio of those SRLGs which are different in M_r^p and M_r^s, i.e. $|M_r^p \triangle M_r^s| / |M_r^p \cup M_r^s|$.

M_r^s) as a similarity measure: if $\mathcal{M}(r)$ is close to 1, it means the two lists are very different, while if it is close to 0, it means there are few differences. We set $r = 8$ to be a bit larger than the half of the diameter of the current network, $r = 0$ to be a small radius, the rest of the r values were linearly interpolated.

Fig. 5 shows that, while in case of `AboveNet`, M_r^p and M_r^s are almost entirely different for many values of r, the tendency is that $\mathcal{M}(r)$ decreases as the physical size of the network decreases, which nicely fits the intuition. Surprisingly, $\mathcal{M}(r)$ is not 0 for every range r even for `AboveNet/300`, which equals to the case when the approximative network diameter is 104km, `AboveNet/400` (having a diameter of approx. 74km) being the most spread out instance where M_r^p and M_r^s are the same for all investigated r ranges.

As a rule of thumb, we can deduct that the difference between the planar and spherical representation of the network can result in different SRLG lists even in case of networks having a geographic extension as small as 100km.

6 | CONCLUSION

We investigated the problem of generating SRLG lists of networks. We found that the known precise low-polynomial SRLG generating techniques can be modified in order to fit the spherical geometry, allowing us to generate SRLG lists with more precision. A framework of easy-to-implement approximate algorithms for determining the SRLG lists in both planar and spherical representation was also presented.

In our experience, SRLG lists generated using the spherical representation of the networks are different from the planar ones, and also they tend to be longer, especially in case of extreme geographical extension. In case of our implementation, enumerating SRLG lists in case of spherical representation was typically 2 times slower than in the planar case. The difference between the planar and spherical representation of the network can result in different SRLG lists even in case of networks having a geographic extension as small as 100km.

While in most of our study we supposed the disasters destroy the network in an area of a circular disk, some results were generalized to essentially arbitrary disaster shapes.

.1 | Determining Smallest Enclosing Disk of Line Segments or Geodesics in $O(1)$

Proof of Lemma 3:

Proof For planar geometry, this problem is already solved, see Thm. 3 of paper [25]. It remains to prove it in case of spherical embedding.

Let e_1, e_2, e_3 be three geodesics on the sphere. The endpoints (p_{i1}, p_{i2}) are given by Cartesian coordinates (x_{i1}, y_{i1}, z_{i1}), (x_{i2}, y_{i2}, z_{i2}). Let p_{i3} be an arbitrary point inside e_i. Points p_{i1}, p_{i2} and p_{i3} determine the great circle on sphere containing geodesic e_i.

We will project geometric objects on the sphere to the plane using the stereographic projection from the north pole, which has the property that the image of a spheric circle will be a circle on the plane, or in special case, if it contains the north pole, its image is a line [22]. Note that for the sake of simplicity it is assumed that the no great circle investigated crosses the north pole.

Projecting the 9 spherical points onto the plane we receive q_{ij} points given by Cartesian coordinates $(x_{ij}, y_{ij}, z_{ij}) \rightarrow q_{ij} = \left(\frac{x_{ij}}{1-z_{ij}}, \frac{y_{ij}}{1-z_{ij}}\right)$. We denote the images of e_1, e_2, e_3 by arcs f_1, f_2, f_3. Calculating the radius and center point of the containing circle c_i for arc f_i requires constant number of coordinate geometric steps. Let $(x_1, y_1), (x_2, y_2), (x_3, y_3)$ and r_1, r_2, r_3 be the Cartesian coordinates of the center of containing circles, and radiuses, respectively.

The smallest enclosing disk c_H on the sphere has an image c'_H on the plane. However the parameters of c'_H are different from the parameters of c_H, the images of the fitting points of c_H and e_i are the fitting points of c'_H and f_i. That inspires the plan to find all the fitting circles of f_i (i.e. those which have exactly 1 common point with each f_i or which have 1 common point with 2 of them and containing the third) on the plane, project them back onto sphere and select the minimal among them, as that is the minimal enclosing disk of e_1, e_2, e_3. Thus we need to find the potential best fitting circles in the plane.

It is possible that the disk fits for two arcs and include some points of the third. We can choose two arbitrary arcs in 3 ways. Choosing f_1, f_2 we must calculate the distance of the two arcs and use it as the diameter of the potential disk. On each arc, the distance is determined by an inside point or one of the boundary points. Calculating the distance of two points, a point and a circle or two circles have both constant complexity. So, in this case, $3 \cdot 3^2 \cdot O(1)$ calculation required.

If the smallest disk touches all of the arcs there are also more different cases. Each arc can be touched on a boundary point or on an inside point (3^3 cases). Fortunately fitting a circle is already solved in all of the cases and called problems of Apollonius[4].

If the smallest enclosing disk touches all three arcs f_1, f_2 and f_3, we have three cases for each arc f_i: the disk either touches the arc in an interior point or at one of its endpoints. In the former case let (x_1, y_1) and r_i be the Cartesian coordinates of center point and radius of the containing circle of arc f_i, respectively. In the latter case, let (x_1, y_1) be coordinates of the endpoint itself, while let r_i be 0. Numbers s_1, s_2 and s_3 are $+/-1$ representing that the fitting circle touches on the outside or on the inside of the containing circles of c_1, c_2 and c_3 (2^3 different possibility to be checked on each case). Parameters x_s, y_s and r_s of the fitting C circle can be calculated by solving the following equation system[10]:

$$(x_s - x_1)^2 + (y_s - y_1)^2 = (r_s - s_1 \cdot r_1)^2$$
$$(x_s - x_2)^2 + (y_s - y_2)^2 = (r_s - s_2 \cdot r_2)^2$$
$$(x_s - x_3)^2 + (y_s - y_3)^2 = (r_s - s_3 \cdot r_3)^2.$$

The system in quadratic, thus it can be solved by constant number of arithmetic calculations. The complexity of these calculations all together are $3^3 \cdot 2^3 \cdot O(1)$.

After finding the $3^3 \cdot 2^3 + 3 \cdot 3^2$ possible minimal disks, we must project them back to the surface of the sphere. We are allowed to use only the two endpoints of an arbitrary diameter from each possible circle. This requires $2 \cdot 3^5$ number of coordinate transformations $(x, y) \rightarrow \left(\frac{2x^2}{1+x^2+y^2}, \frac{2y^2}{1+x^2+y^2}, \frac{-1+x^2+y^2}{1+x^2+y^2}\right)$.

Finding the minimal radius of potential disks requires $3^5 - 1$ comparisons between diameters. Using this method the minimal disk for e_1, e_2, e_3 can be determined in $O(1)$ time. However, the algorithm could be improved by using preconceptions for the edges, exclude some possible disks already on the plane instead of transforming back or fixing s_i in case of boundary points. Note that only a constant number of basic arithmetic functions ($+, -, \times, /, \sqrt{}$) were used during the computation.

REFERENCES

[1] The internet topology zoo. URL: `http://www.topology-zoo.org/dataset.html`.

[2] Pankaj K Agarwal, Alon Efrat, Shashidhara K Ganjugunte, David Hay, Swaminathan Sankararaman, and Gil Zussman. The resilience of wdm networks to probabilistic geographical failures. *IEEE/ACM Transactions on Networking (TON)*, 21(5):1525–1538, 2013.

[3] National Research Council. *Severe Space Weather Events: Understanding Societal and Economic Impacts: A Workshop Report*. The National Academies Press, Washington, DC, 2008. URL: `https://www.nap.edu/catalog/12507/severe-space-weather-events-understanding-societal-and-economic-impacts-a`, http://dx.doi.org/10.17226/12507 `doi:10.17226/12507`.

[4] H. S. M. Coxeter. The problem of Apollonius. In *The American Mathematical Monthly*, volume 75, pages 5–15.

[5] Mark De Berg, Marc Van Kreveld, Mark Overmars, and Otfried Cheong Schwarzkopf. *Computational geometry*. Springer, 2000.

[6] Ferhat Dikbiyik, Massimo Tornatore, and Biswanath Mukherjee. Minimizing the risk from disaster failures in optical backbone networks. *Journal of Lightwave Technology*, 32(18):3175–3183, 2014.

[7] M Todd Gardner and Cory Beard. Evaluating geographic vulnerabilities in networks. In *IEEE Int. Workshop Technical Committee on Communications Quality and Reliability (CQR)*, pages 1–6, 2011.

[8] Ori Gerstel, Masahiko Jinno, Andrew Lord, and SJ Ben Yoo. Elastic optical networking: A new dawn for the optical layer? *Communications Magazine, IEEE*, 50(2):s12–s20, 2012.

[9] T. Gomes, J. Tapolcai, C. Esposito, D. Hutchison, F. Kuipers, J. Rak, A. de Sousa, A. Iossifides, R. Travanca, J. André, L. Jorge, L. Martins, P. O. Ugalde, A. Pašić, D. Pezaros, S. Jouet, S. Secci, and M. Tornatore. A survey of strategies for communication networks to protect against large-scale natural disasters. In *2016 8th International Workshop on Resilient Networks Design and Modeling (RNDM)*, pages 11–22, Sept 2016. http://dx.doi.org/10.1109/RNDM.2016.7608263 `doi:10.1109/RNDM.2016.7608263`.

[10] Coaklay G.W. Analytical solutions of the ten problems in the tangencies of circles; and also of the fifteen problems in the tangencies of spheres. In *The Mathematical Monthly*, volume 2, pages 116–126.

[11] M Farhan Habib, Massimo Tornatore, Marc De Leenheer, Ferhat Dikbiyik, and Biswanath Mukherjee. Design of disaster-resilient optical datacenter networks. *Journal of Lightwave Technology*, 30(16):2563–2573, 2012.

[12] Isil Burcu Barla Harter, Dominic Schupke, Marco Hoffmann, Georg Carle, et al. Network virtualization for disaster resilience of cloud services. *Communications Magazine, IEEE*, 52(12):88–95, 2014.

[13] John Heidemann, Lin Quan, and Yuri Pradkin. *A preliminary analysis of network outages during hurricane Sandy*. University of Southern California, Information Sciences Institute, 2012.

[14] A. Kushwaha, D. Kapadia, A. Gumaste, and A. Somani. Designing multi-layer provider networks for circular disc failures. In *International Conference on Optical Network Design and Modeling (ONDM)*, Dublin, Ireland, May 2018.

[15] G. S. Lakhina and B. T. Tsurutani. Geomagnetic storms: historical perspective to modern view. *Geoscience Letters*, 2016.

[16] Xuelian Long, David Tipper, and Teresa Gomes. Measuring the survivability of networks to geographic correlated failures. *Optical Switching and Networking*, 14:117–133, 2014.

[17] Biswanath Mukherjee, M Habib, and Ferhat Dikbiyik. Network adaptability from disaster disruptions and cascading failures. *Communications Magazine*, 52(5):230–238, 2014.

[18] Hyeon-Suk Na, Chung-Nim Lee, and Otfried Cheong. Voronoi diagrams on the sphere. *Computational Geometry*, 23(2):183–194, 2002.

[19] Sebastian Neumayer, Gil Zussman, Reuven Cohen, and Eytan Modiano. Assessing the vulnerability of the fiber infrastructure to disasters. *IEEE/ACM Transactions on Networking (TON)*, 19(6):1610–1623, 2011.

[20] Evanthia Papadopoulou and Maksym Zavershynskyi. The higher-order Voronoi diagram of line segments. *Algorithmica*, 74(1):415–439, 2016.

[21] J. Rak, D. Hutchison, E. Calle, T. Gomes, M. Gunkel, P. Smith, J. Tapolcai, S. Verbrugge, and L. Wosinska. RECODIS: Resilient communication services protecting end-user applications from disaster-based failures. In *18th International Conference on Transparent Optical Networks (ICTON)*, July 10-14 2016. Invited paper. URL: http://ieeexplore.ieee.org/stamp/stamp.jsp?tp=&arnumber=7550596&isnumber=7550246.

[22] B.A. Rozenfeld and N. D. Sergeeva. *Stereographic projection*. Mir Publisher, Moscow, USSR, 1977.

[23] J. P. Snyder. *Map projections: A working manual*. U.S. Government Printing Office, 1987.

[24] Rodrigo Souza Couto, Stefano Secci, Miguel Mitre Campista, Kosmalski Costa, and Luis Maciel. Network design requirements for disaster resilience in iaas clouds. *Communications Magazine, IEEE*, 52(10):52–58, 2014.

[25] János Tapolcai, Lajos Rónyai, Balázs Vass, and László Gyimóthi. List of shared risk link groups representing regional failures with limited size. In *Proc. IEEE INFOCOM*, Atlanta, USA, may 2017.

[26] János Tapolcai, Balázs Vass, Zalán Heszberger, József Biró, David Hay, Fernando A. Kuipers, and Lajos Rónyai. A tractable stochastic model of correlated link failures caused by disasters. In *Proc. IEEE INFOCOM*, Honolulu, USA, April 2018.

[27] Stojan Trajanovski, Fernando Kuipers, Piet Van Mieghem, et al. Finding critical regions in a network. In *IEEE Conference on Computer Communications Workshops (INFOCOM WKSHPS)*, pages 223–228. IEEE, 2013.

[28] Stojan Trajanovski, Fernando A Kuipers, Aleksandar Ilić, Jon Crowcroft, and Piet Van Mieghem. Finding critical regions and region-disjoint paths in a network. *IEEE/ACM Transactions on Networking (TON)*, 23(3):908–921, 2015.

[29] B. Vass, L. Németh, A. de Sousa, M. Zachariasen, and J. Tapolcai. Vulnerable regions of networks on sphere. In *Int. Workshop on Resilient Networks Design and Modeling (RNDM)*, Longyearbyen, Svalbard, Norway, 2018.

[30] Balázs Vass, Erika Bérczi-Kovács, and János Tapolcai. Enumerating shared risk link groups of circular disk failures hitting k nodes. In *Proc. International Workshop on Design Of Reliable Communication Networks (DRCN)*, Munich, Germany, march 2017.